

Supplementary Information

Facile construction of covalent triazine framework as anode for ultra-long cycle life sodium-ion batteries

Ying Huang,^{†a} Suping Chen,^{†a} Tao Yang,^a Xijun Xu,^{*a} Fangkun Li,^b Jujun Yuan,^{*c} Sihuan Tang,^a Yanping Huo,^{a,d} and Jun Liu^{*b}

Experimental Section

Materials

All the materials and solvents were purchased from commercial sources without further purification. Trifluoromethanesulfonic acid ($\text{CF}_3\text{SO}_3\text{H}$) was purchased from Energy Chemical. 1,4-benzeneddicarbonitrile (monomer), N-dimethylformamide (DMF), dichloromethane (CH_2Cl_2), and ethanol were purchased from Aladdin. $\text{Na}_3\text{V}_2(\text{PO}_4)_3$ was purchased from Kejing Zhida Technology Co., Ltd (Shenzhen, China).

Preparation of CTF powders

The CTF was prepared in a mixture solution according to the previous report.^[1] Typically, 40 mL of $\text{CF}_3\text{SO}_3\text{H}$ was added to a pre-dried flask, and 80 mg of 1,4-dicyanobenzene was previously dissolved in 400 mL CH_2Cl_2 , respectively. Afterwards, the monomer solution was transferred into a dropping funnel and was added dropwise to the flask at a temperature of 100 °C for 1 hour. Because of the immiscibility of the CH_2Cl_2 and $\text{CF}_3\text{SO}_3\text{H}$ solvents, triggering the polymerization by the cyclotrimerization reaction. The reaction was kept for another 20 min to promote the complete reaction conversion. The solution was then quenched by ethanol, followed by filtration. The final product was obtained after washing with ethanol and N, N-dimethylformamide (DMF) several times and drying in a vacuum oven at 80 °C for 4 hours.

Materials Characterization.

The chemical structure of the samples was characterized by Fourier-Transform Infrared (FT-IR) spectroscopy (Nicolet 6700 FTIR 3) in attenuated total reflectance (ATR) mode in the range of 400~4000 cm^{-1} . Powder structural information was obtained by X-ray diffraction (XRD) using $\text{Cu}-\text{K}\alpha$ radiation. The morphology, microstructure, and elemental composition of the synthesized materials were examined using field-emission scanning electron microscopy (FESEM, Hitachi SU8220). Field emission transmission electron microscopy (Thermo Talos F200S) with an acceleration voltage of 200 kV was utilized to reveal the morphology, size, and structure of CTF.

Electrochemical measurements

To prepare the working electrodes, the active material (CTF), conductive carbon black

(Super P), and binder (sodium alginate, SA) were thoroughly mixed in a mass ratio of 6:3:1. Deionized water was added during mixing to form a homogeneous slurry, which was then coated onto carbon-coated Al foil, punched into 12 mm diameter discs, and vacuum-dried at 80 °C for 12 hours. The mass loading of active material on each copper disc was approximately 1.0~1.3 mg. The working electrodes were paired with sodium metal and assembled into CR2025 coin cells in an argon-filled glove box for electrochemical testing. 1M NaPF₆ in ethylene glycol dimethyl ether (DME) was used as the electrolyte. A porous glass fiber membrane (Whatman GF/D) was used as the separator. Galvanostatic charge/discharge (GCD) profiles, galvanostatic intermittent titration technique (GITT), and cycling performance tests were carried out in the voltage range of 0.01–2.1 V using a LAND CT2003A battery testing system. Specific capacities were calculated based on the total mass of active material. Electrochemical impedance spectroscopy (EIS, frequency range: 10⁶ Hz to 0.1 Hz) and cyclic voltammetry (CV, scan rate: 0.1–1.0 mV s⁻¹) were conducted on electrochemical workstations (Gamry and CHI760D) within the voltage range of 0.01~2.1 V. For the full cell, the commercial Na₃V₂(PO₄)₃ (NVP) powder was used as a cathode. The NVP powder was mixed with Super P and polyvinylidene fluoride (PVDF) with a mass ratio of 8:1:1 and dispersed in N-methyl pyrrolidone (NMP) to form a slurry. Then, the slurry was cast on carbon-coated aluminum foil and dried under vacuum at 80°C overnight. GCD testing for the full cell within the voltage range of 1~3.3 V. The current density of the GITT test was 0.1 A g⁻¹. The calculation procedure follows the formula below.

$$D = \frac{4}{\pi \tau} \times \left(\frac{m_B V_M}{M_B S} \right)^2 \times \left(\frac{\Delta E_S}{\Delta E_t} \right)^2$$

Where m_B and M_B are the mass and molecular weight of the anodes, V_M is the molar volume of these anodes, and S is the electrode surface area, ΔE_S and ΔE_t represent the potential differences during the different stages.

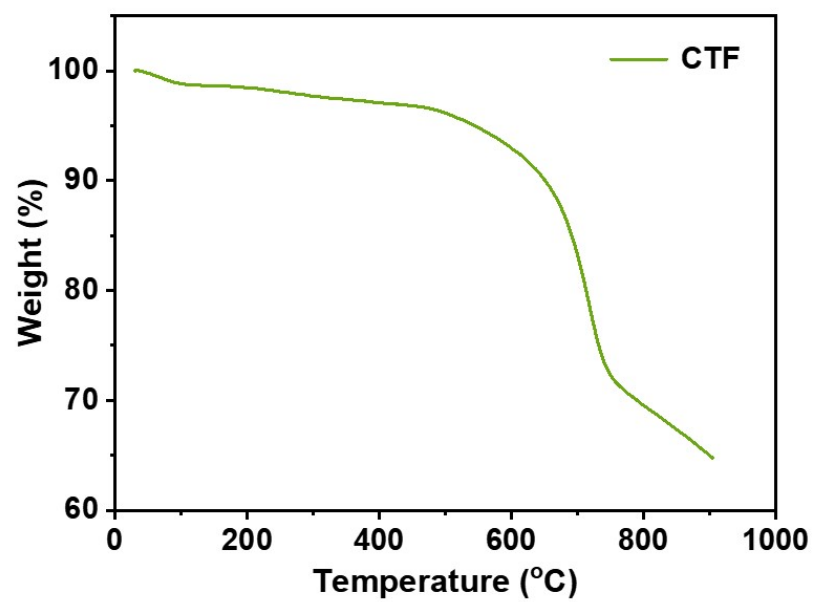


Figure S1 TAG result of CTF.

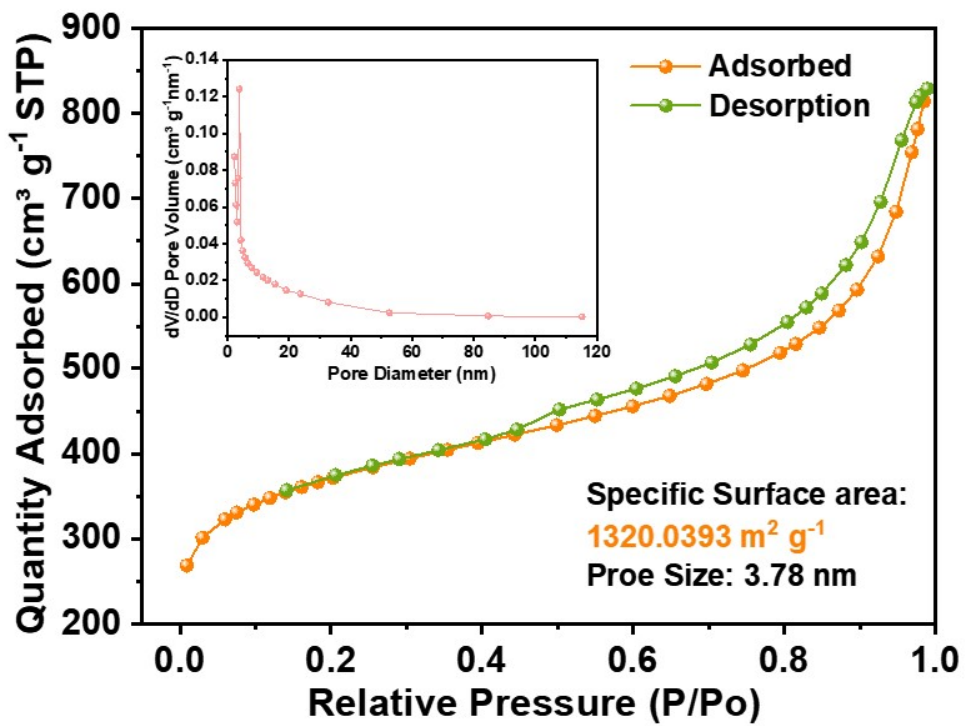


Figure S2 N_2 sorption isotherms of CTF.

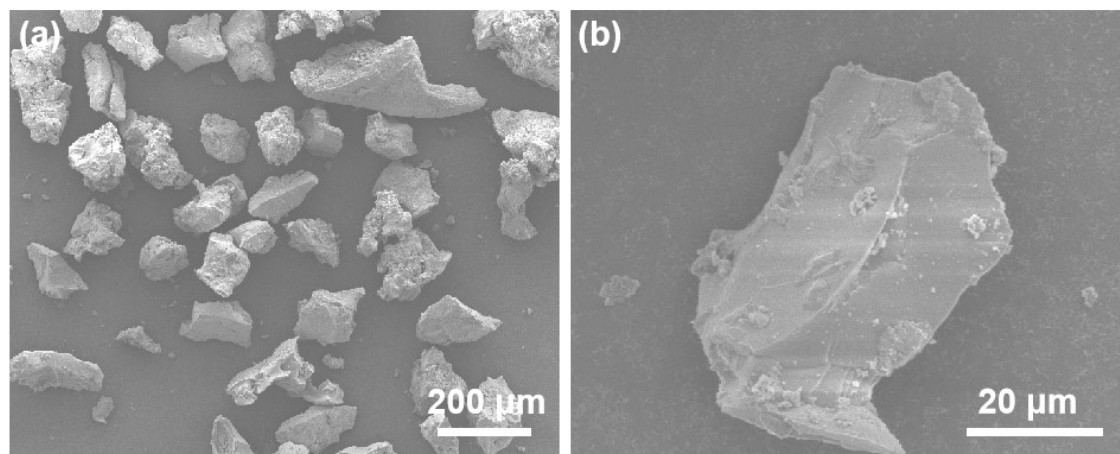


Figure S3 (a,b) SEM images of the CTF.

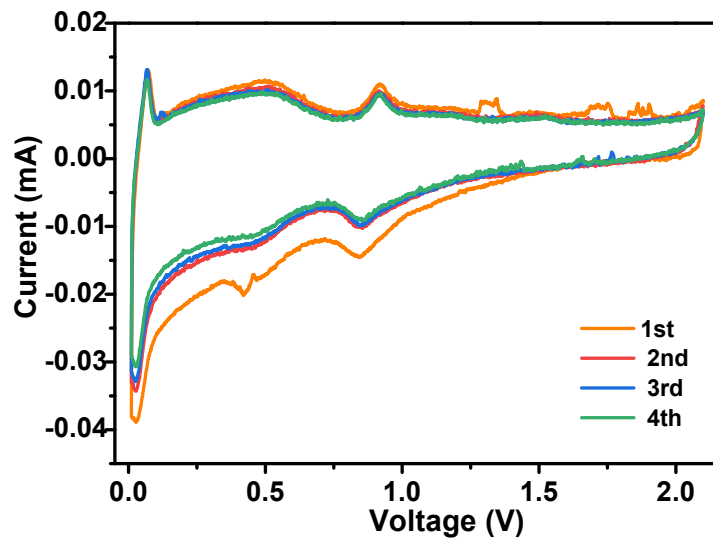


Figure S4 CV curves of CTF anode at 0.1 mV s^{-1} within $0.01 \text{~} 2.1 \text{ V}$

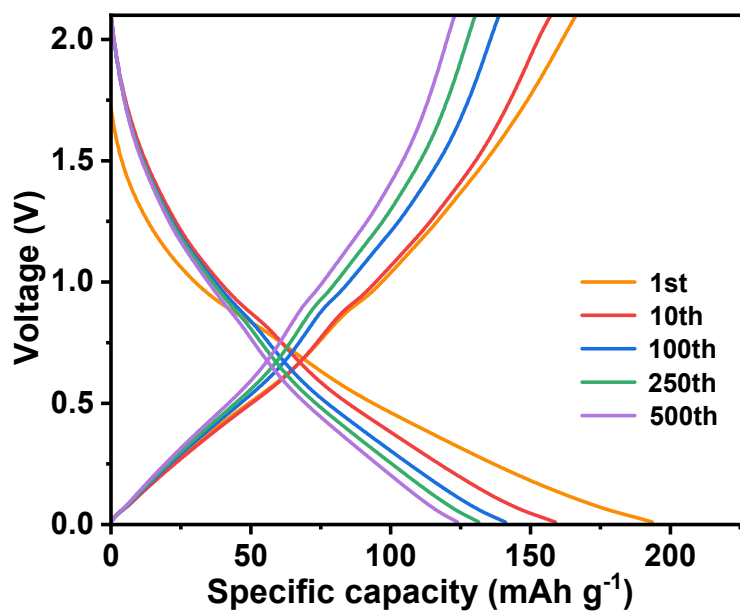


Figure S5 Voltage-capacity profiles of CTF anode at 1st, 10th, 100th, 250th, and 500th cycles under 0.1 A g⁻¹.

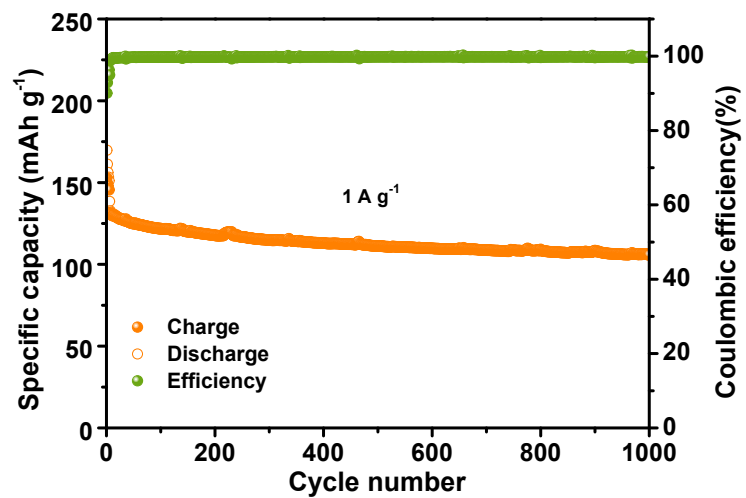


Figure S6 Long cycling performance of the CTF anode at 1.0 A g^{-1} .

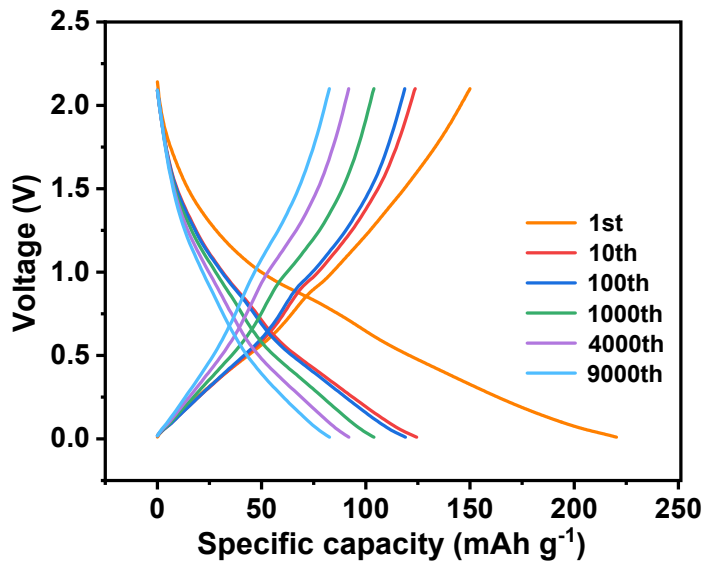


Figure S7 Voltage-capacity profiles of CTF anode at 1st, 10th, 100th, 1000th, 4000th, and 9000th cycles under 2.0 A g⁻¹.

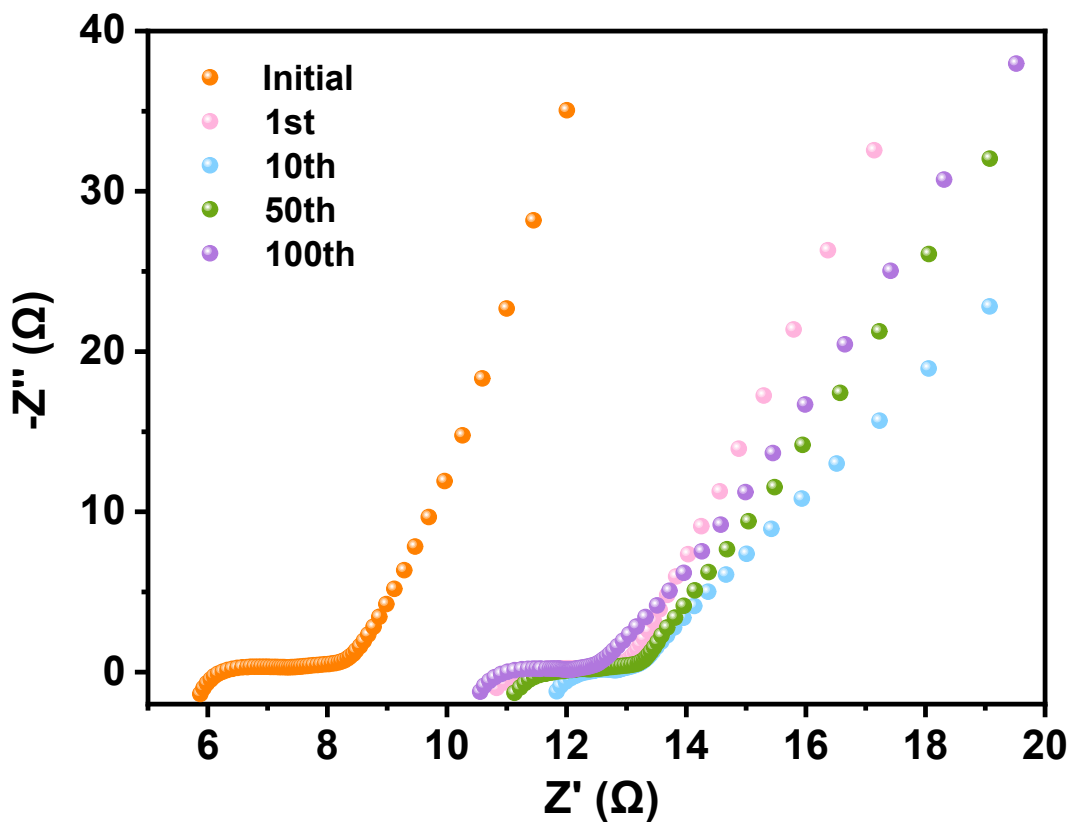


Figure S8 Nyquist plots of the CTF anode at different cycling stages (Initial, 1st, 10th, 50th, and 100th cycles).

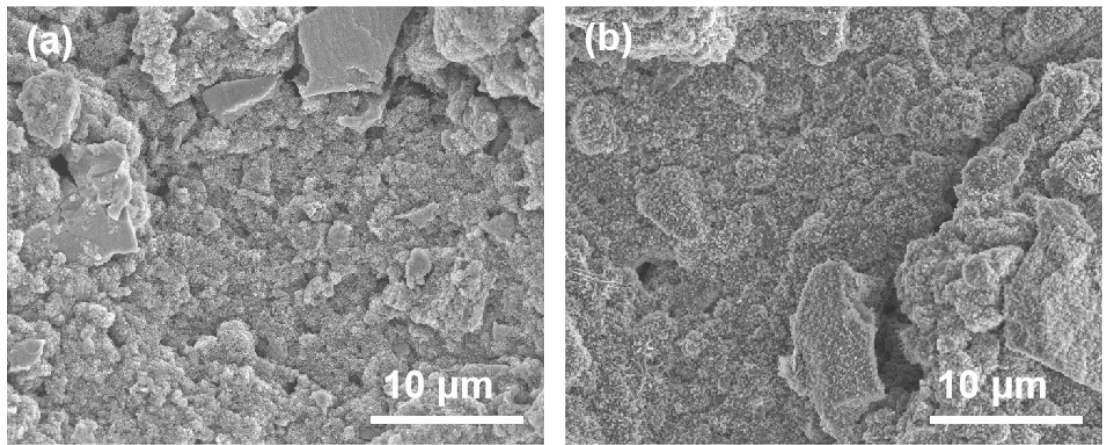


Figure S9 The SEM images of the CTF anode (a) before and (b) after 30 cycles at 0.1A g⁻¹.

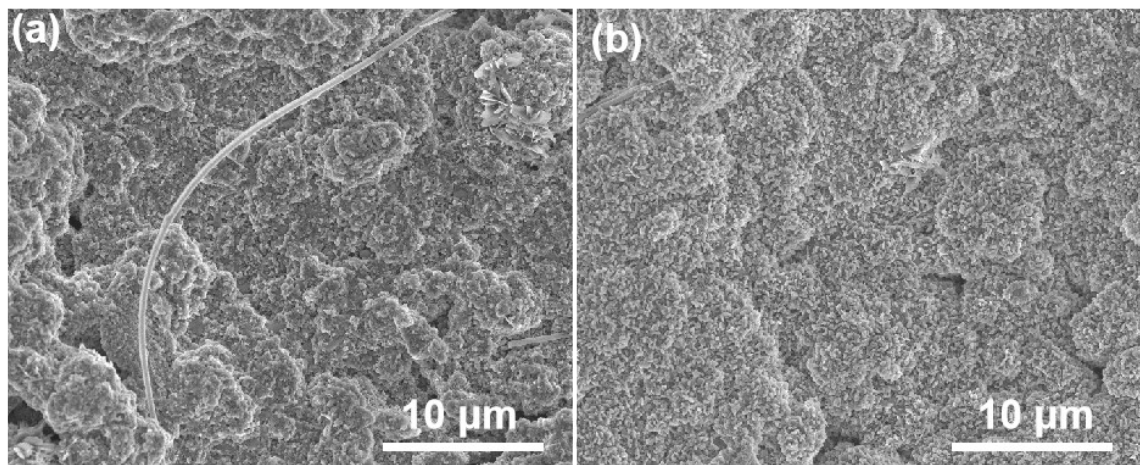


Figure S10 The SEM images of the CTF anode at different states: (a) fully charged (2.1V), and (b) fully discharged (0.01 V).

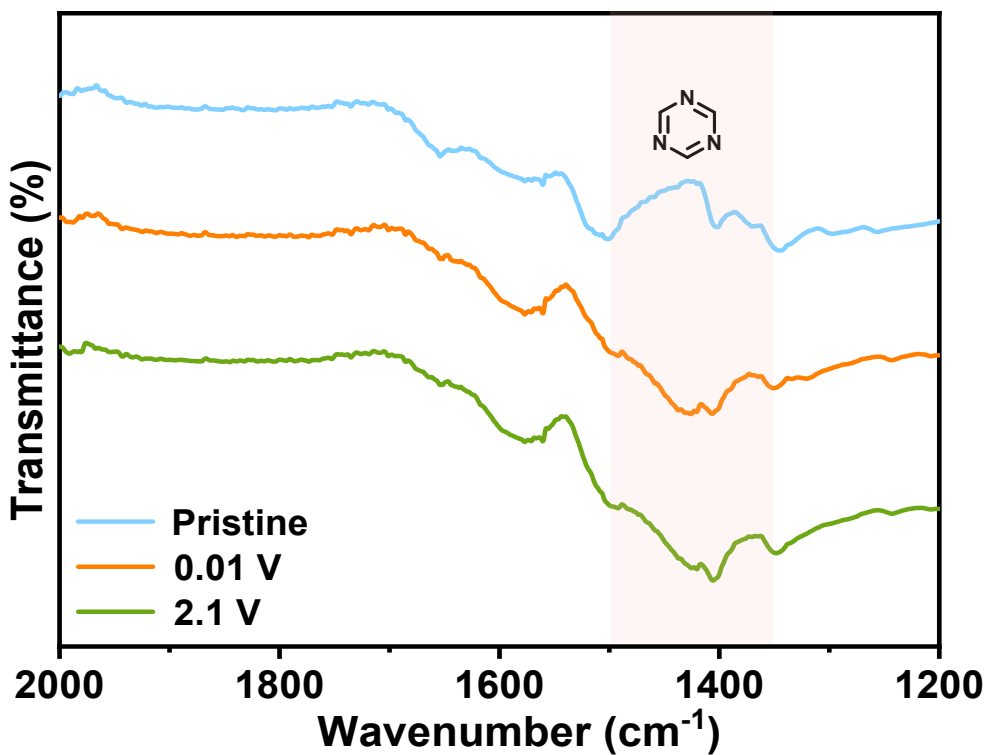


Figure S11 The FTIR results of the CTF anode at pristine fully charged (2.1V) and (b) fully discharged (0.01 V) states.

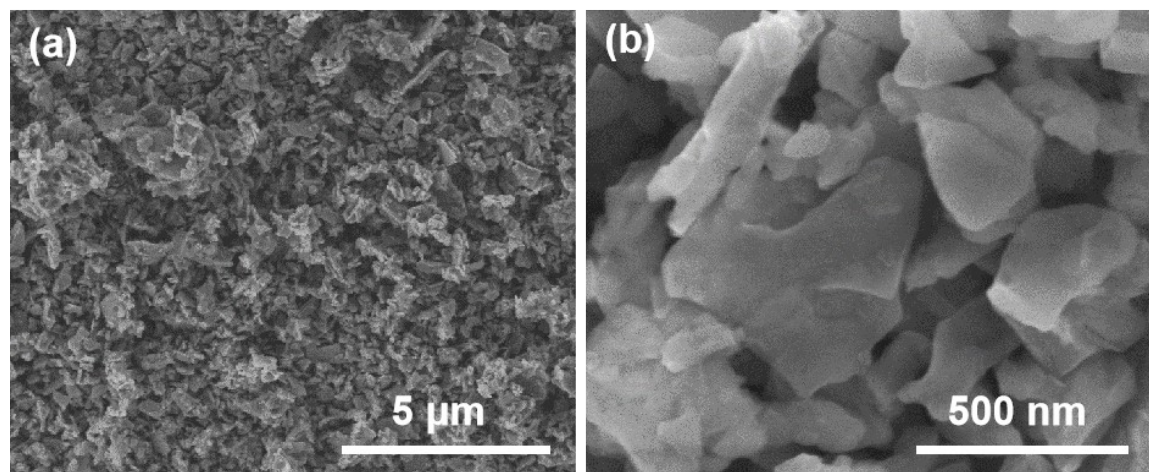


Figure S12 (a) low-magnification and (b) high-magnification SEM images of the $\text{Na}_3\text{V}_2(\text{PO}_4)_3$

Table S1. The electrochemical performances comparision of this anode with reported covalent organic frameworks for SIBs.

Electrode Materials	Current density (mA g ⁻¹)	Specific capacity (mA h g ⁻¹)	Cycle number (cycles)	Voltage region (V)	Reference
Millimeter-size CTF	1000	163	1200	0.01–2.5	[2]
2D Polymer	1000	198	1200	0.01–2.5	[2]
IISERP-COF16	500	~20	500	0.05–3.0	[3]
IISERP-COF17	1000	~85	500	0.05–3.0	[3]
IISERP-COF18	1000	340	1400	0.05–3.0	[3]
TFPB-TAPT COF	30	125	500	0.01–3.0	[4]
DAAQ–HCCP	2000	72	1000	0.1–2.0	[5]
BCOF-1	1200	156	400	0.01–3.0	[6]
E-FCTF	100	220	200	0.005–2.7	[7]
FCTF	100	106	200	0.005–2.7	[7]
CTF-0, CTF-1	100	~100	300	0.01–3.0	[8]
This work	100	123.9	500	0.05–2.1	This work
	2000	82.6	9000	0.05–2.1	

Reference

- [1] J. Liu, W. Zan, K. Li, Y. Yang, F. Bu and Y. Xu, *J. Am. Chem. Soc.*, 2017, **139**, 11666-11669.
- [2] J. Liu, P. Lyu, Y. Zhang, P. Nachtigall and Y. Xu, *Adv. Mater.*, 2018, **30**, 1705401.
- [3] S. Haldar, D. Kaleeswaran, D. Rase, K. Roy, S. Ogale and R. Vaidhyanathan, *Nanoscale Horiz.*, 2020, **5**, 1264-1273.
- [4] B. C. Patra, S. K. Das, A. Ghosh, P. Moitra, M. Addicoat, S. Mitra, A. Bhaumik, S. Bhattacharya and A. Pradhan, *J. Mater. Chem. A*, 2018, **6**, 16655-16663.
- [5] M.-M. Hu, H. Huang, Q. Gao, Y. Tang, Y. Luo, Y. Deng and L. Zhang, *Energy Fuels*, 2020, **35**, 1851-1858.
- [6] M. K. Shehab and H. M. El-Kaderi, *ACS Appl. Mater. Interfaces*, 2024, **16**, 14750-14758.
- [7] H. Zhang, W. Sun, X. Chen and Y. Wang, *ACS Nano*, 2019, **13**, 14252-14261.
- [8] S.-Y. Li, W.-H. Li, X.-L. Wu, Y. Tian, J. Yue and G. Zhu, *Chem. Sci.*, 2019, **10**, 7695-7701.